Magnetic structure of the noncentrosymmetric perovskites $PbVO_3$ and $BiCoO_3$: Theoretical analysis

I. V. Solovyev*
National Institute for Materials Science, 1-2-1 Sengen, Tsukuba, Ibaraki 305-0047, Japan
(Received 21 December 2011; published 21 February 2012)

It is well known that, if a crystal structure has no inversion symmetry, it may allow for Dzyaloshinskii-Moriya magnetic interactions, operating between different crystallographic unit cells, which, in turn, should lead to the formation of long-periodic spin-spiral structures. Such a behavior is anticipated for two simple perovskites $PbVO_3$ and $BiCoO_3$, crystallizing in the noncentrosymmetric tetragonal $P4mm$ structure. Nevertheless, we argue that, in reality, $PbVO_3$ and $BiCoO_3$ should behave very differently. Due to the fundamental Kramers degeneracy for the odd-electron systems, $PbVO_3$ has no single-ion anisotropy. Therefore, the ground state of $PbVO_3$ indeed will be the spin spiral with the period of about 100 unit cells. However, the even-electron $BiCoO_3$ has a large single-ion anisotropy, which locks this system in the collinear easy-axis C-type antiferromagnetic ground state. Our theoretical analysis is based on the low-energy model, derived from the first-principles electronic structure calculations.

DOI: 10.1103/PhysRevB.85.054420 PACS number(s): 75.25.−j, 75.30.−m, 77.80.−e, 71.10.−w

I. INTRODUCTION

Magnetic materials, crystallizing in the noncentrosymmetric structure, have attracted a great deal of attention. The lack of inversion symmetry gives rise to the ferroelectric activity. If the latter property is combined with the magnetism, the system becomes multiferroic, which has many merits for the next generation of electronic devices. For example, one can control the magnetization by applying the electric field and vice versa. The canonical example of such materials is $BiFeO_3$, which simultaneously possesses a high magnetic transition temperature (about 640 K) and a high ferroelectric Curie temperature (about 1090 K).[1]

Recently fabricated $PbVO_3$ and $BiCoO_3$ belong to the same category. They crystallize in the noncentrosymmetric tetragonal $P4mm$ structure (Fig. 1).[2,3] $BiCoO_3$ is an antiferromagnetic (AFM) insulator of the C type with the Néel temperature of about 470 K.[3] The experimental information about $PbVO_3$ is rather controversial.[4,5] The magnetic susceptibility has a broad maximum around 200 K, which might be the sign of an antiferromagnetism. On the other hand, no long-range magnetic order was found down to 1.8 K in the neutron-diffraction experiments. Nevertheless, the analysis of neutron data depends on the model of magnetic structure, which typically is assumed in the process of interpretation of these data. Finally, the experimental studies of $PbVO_3$ may be hampered by possible defects in the sample.[5]

According to first-principles electronic structure calculations, both $PbVO_3$ and $BiCoO_3$ are expected to have the C-type AFM ground state, although in $PbVO_3$, it is nearly degenerate with the G-type AFM state.[6,7] Giant electric polarization (more than 15 $\mu C/cm^2$) was predicted theoretically for both $PbVO_3$ and $BiCoO_3$,[6] which spurred additional interest in these systems.

Nevertheless, the violation of the inversion symmetry gives rise to a number of interesting effects, which currently are not accessible by the first-principles electronic structure calculations, simply due to their complexity. One of them is a complex magnetic ordering, caused by antisymmetric Dzyaloshinskii-Moriya interactions of the relativistic origin. In the noncentrosymmetric systems, these interactions can operate between different crystallographic unit cells, thus, driving the formation of long-periodic spin-spiral superstructures.[8] Particularly, the idea of the spin-spiral order in various oxide materials has attracted much attention recently in the context of their multiferroic behavior and was proposed as one of the possible origins of such behavior.[9]

In this paper, we address some basic issues of the formation of the spin-spiral states in $PbVO_3$ and $BiCoO_3$. We argue that, despite similarities in the lattice distortion and population of the crystal-field levels, these two compounds behave very differently. Particularly, we show that the long-periodic spin spiral is a probable candidate for the magnetic ground state of $PbVO_3$ where, due to the fundamental Kramers degeneracy, the single-ion anisotropy does not exist. On the contrary, the spin-spiral state in $BiCoO_3$ (for which the Kramers theorem is no longer applicable) is suppressed by the single-ion anisotropy, which reinforces the formation of the easy-axis collinear C-type AFM ground state. Our analysis is based on the low-energy model, derived from the first-principles electronic structure calculations. In this sense, this is the continuation of our previous papers, devoted to the realistic modeling of complex oxide materials and other strongly correlated systems.[10–12]

The rest of the paper is organized as follows. In Sec. II, we briefly discuss the construction of the low-energy model (in our case—the multiorbital Hubbard model) on the basis of first-principles electronic structure calculations. All model parameters are collected in the Supplemental Material.[13] Section III A is devoted to the semiquantitative analysis of the spin model, which can be derived from the multiorbital Hubbard model. Particularly, we consider the formation of incommensurate spin-spiral states, resulting from the competition between isotropic exchange and Dzyaloshinskii-Moriya interactions and explain the main difference in the behavior of the single-ion anisotropy in $PbVO_3$ and $BiCoO_3$. In Sec. III B, we present results of the extensive search for the long-periodic spin-spiral states, which are based on the solution of the electronic Hubbard model in the Hartree-Fock (HF) approximation. Finally, in Sec. IV, we briefly summarize the main results.

II. CONSTRUCTION OF THE LOW-ENERGY MODEL

The magnetic properties of $PbVO_3$ and $BiCoO_3$ are determined mainly by the behavior of the $3d$ bands located near the Fermi level. Therefore, the basic idea of our approach is to construct an effective low-energy model, formulated in the Wannier basis for the $3d$ bands and to solve it by using model techniques. More specifically, we adopt the form of the multiorbital Hubbard model on the lattice of transition-metal sites,

$$\hat{\mathcal{H}} = \sum_{ij}\sum_{\alpha\alpha'} t_{ij}^{\alpha\alpha'}\hat{c}_{i\alpha}^{\dagger}\hat{c}_{j\alpha'} + \frac{1}{2}\sum_{i}\sum_{\{\alpha\}} U_{\alpha\alpha'\alpha''\alpha'''}\hat{c}_{i\alpha}^{\dagger}\hat{c}_{i\alpha''}^{\dagger}\hat{c}_{i\alpha'}\hat{c}_{i\alpha'''}, \tag{1}$$

where we use the shorthand notations, according to which, each greek symbol stands for the combination of spin ($s = \uparrow$ or $\downarrow$) and orbital ($m = xy$, yz, $3z^2 - r^2$, zx, or $x^2 - y^2$) indices. All parameters of the model Hamiltonian can be derived in an *ab initio* fashion on the basis of first-principles electronic structure calculations. For instance, the one-electron part $t_{ij}^{\alpha\alpha'}$ was obtained by using the downfolding procedure, and the Coulomb (and exchange) interactions $U_{\alpha\alpha'\alpha''\alpha'''}$ were obtained by combining the constrained density-functional theory with the random-phase approximation (RPA). The method is discussed in the literature, and for details, the reader is referred to Ref. 10. Recent applications to multiferroic compounds can be found in Refs. 11 and 12. In all calculations, we use the experimental parameters of the crystal structure, reported in Refs. 2 and 3.

Without spin-orbit interaction (SOI), $t_{ij}^{\alpha\alpha'}$ is diagonal with respect to the spin indices $t_{ij}^{\alpha\alpha'} \equiv t_{ij}^{mm'}\delta_{ss'}$. The site-diagonal part of $\hat{t}_{ij} = \|t_{ij}^{mm'}\|$ describes the crystal-field effects, whereas, the off-diagonal part stands for transfer integrals. It is also important to remember that the local symmetry around the transition-metal sites is $4mm$ (in the Hermann-Mauguin notations or C_{4v} in the Schoenflies notations). The coordinate frame is explained in Fig. 1.

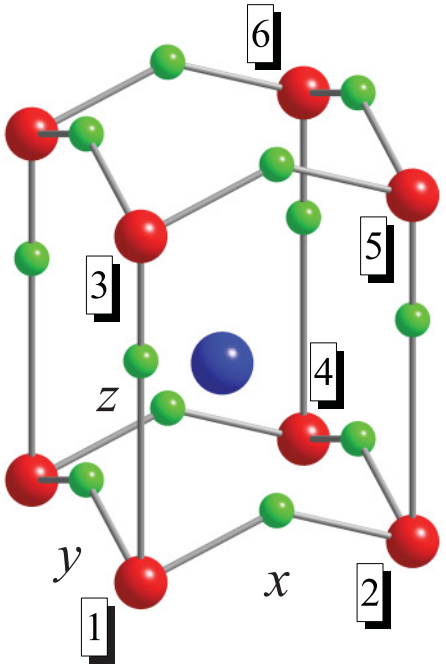

FIG. 1. (Color online) Fragment of the crystal structure of $BiCoO_3$. The Bi atoms are indicated by the big blue (dark) spheres, the Co atoms are indicated by the medium red (dark gray) spheres, and the oxygen atoms are indicated by the small green (light gray) spheres.

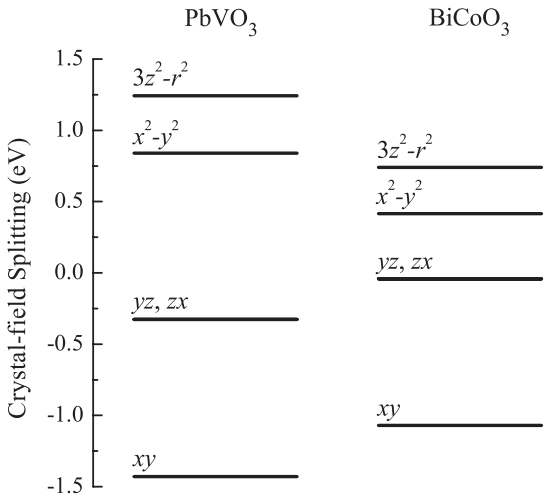

FIG. 2. Scheme of the crystal-field splitting in $PbVO_3$ (left) and $BiCoO_3$ (right).

The crystal field stabilizes the xy orbitals (Fig. 2). The splitting between the xy and the following, after them, yz and zx orbitals are about 1 eV both for $PbVO_3$ and $BiCoO_3$. The $x^2 - y^2$ and $3z^2 - r^2$ orbitals lie in the higher-energy region (and are substantially higher for $PbVO_3$ in comparison with $BiCoO_3$). Thus, from the viewpoint of the crystal-field splitting, $PbVO_3$ and $BiCoO_3$ are expected to be very similar: $PbVO_3$ has only one d electron, which occupies the xy orbital. $BiCoO_3$ has six d electrons, which obey Hund's rule. Therefore, one of them will occupy the minority spin xy orbital and interact with the spherically symmetric majority-spin electron density, created by remaining five electrons.

The details of transfer integrals can be found in Ref. 13. One of the most interesting features in $\hat{t}_{ij}$ is the appearance of the so-called forbidden hoppings, for example, between $3z^2 - r^2$ and zx orbitals in bond 1-2, which would not exist in the centrosymmetric structure (see Fig. 1 for the notations of atomic sites and the coordinate frame). These transfer integrals have the following form (in meV):

$$\hat{t}_{12} = \begin{pmatrix} -173 & 38 & 0 & 0 & 0 \\ -38 & 44 & 0 & 0 & 0 \\ 0 & 0 & 50 & -116 & 2 \\ 0 & 0 & 116 & 196 & -321 \\ 0 & 0 & 2 & 321 & -262 \end{pmatrix},$$

and

$$\hat{t}_{12} = \begin{pmatrix} -56 & 6 & 0 & 0 & 0 \\ -6 & 38 & 0 & 0 & 0 \\ 0 & 0 & 34 & -48 & -3 \\ 0 & 0 & 48 & 231 & -228 \\ 0 & 0 & -3 & 228 & -164 \end{pmatrix}$$

for $PbVO_3$ and $BiCoO_3$, respectively, in the basis of xy, yz, $3z^2-r^2$, zx, and x^2-y^2 orbitals. The microscopic origin of such forbidden hoppings was considered in Ref. 10. Due to the parity violation, the Wannier orbital, which is formally labeled as "$3z^2-r^2$" has some of the weight of the p_z orbitals and, therefore, can interact with the zx orbitals of the neighboring sites. Such hoppings give rise to the antisymmetric part of $\hat{t}_{ij}$, which is responsible for the appearance of Dzyaloshinskii-Moriya interactions. A similar situation takes place in bonds 1-4 and 1-5. On the contrary, due to the $4mm$ symmetry, the transfer integrals in bond 1-3 are diagonal with respect to the orbital indices (the actual values are $t_{13}^{mm}=-45$, 4, -237, 4, and -21 meV for $PbVO_3$ and $t_{13}^{mm}=-19$, 24, -42, 24, and -34 meV for $BiCoO_3$—other details can be found in Ref. 13). Therefore, the forbidden hoppings do not take place, and Dzyaloshinskii-Moriya interactions vanish.

As for the relativistic SOI, we adopted two schemes. In the first one, we evaluate the SOI only at the transition-metal sites and add it to the site-diagonal part of $t_{ij}^{\alpha\alpha'}$ in the form $\xi\mathbf{LS}$, where $\xi=35$ and 81 meV for $PbVO_3$ and $BiCoO_3$, respectively. Thus, the effects of the SOI are expected to be stronger in $BiCoO_3$: due to large ξ and smaller crystal-field splitting (Fig. 2), which competes with the SOI. As a test, we also tried the second scheme where the SOI was included at all sites on the level of the band-structure calculations, and then, corresponding parameters $t_{ij}^{\alpha\alpha'}$ were derived through the downfolding procedure. For example, this scheme includes the effect of a large SOI on the heavy Pb and Bi elements. The parameters $t_{ij}^{\alpha\alpha'}$, derived in the second scheme, also were used in the HF calculations considered in Sec. III B. However, the equilibrium magnetic structures obtained by using these two sets of parameters $t_{ij}^{\alpha\alpha'}$ were practically identical. Thus, in the following, we discuss only the first case.

The spin dependence of Coulomb matrix elements has the standard form: $U_{\alpha\alpha'\alpha''\alpha'''}=U_{mm'm''m'''}\delta_{ss'}\delta_{s''s'''}$. The details of $U_{mm'm''m'''}$ can be found in Ref. 13. A rough idea about the strength of the matrix elements $U_{mm'm''m'''}$ can be obtained by interpolating them in terms of three characteristic averaged parameters U, J, and B, which would take place in the centrosymmetrical environment of isolated atoms. In these notations, $U=F^0$ is the on-site Coulomb interaction, $J=(F^2+F^4)/14$ is the intra-atomic exchange interaction, and $B=(9F^2-5F^4)/441$ is the nonsphericity, in terms of radial Slater's integrals F^0, F^2, and F^4. In other words, U enforces the charge stability of certain atomic configurations, while J and B are responsible for the Hund rules. The results of such an interpolation are shown in Table I. One clearly can see that the on-site Coulomb repulsion U is strongly screened, especially in $PbVO_3$, while other parameters are close to their atomic values. We use this interpolation only for explanatory purposes, while all practical calculations were performed with actual parameters $U_{mm'm''m'''}$ reported in Ref. 13. The deviation in $U_{mm'm''m'''}$ from the centrosymmetric form is quite strong. For example, in the case of $BiCoO_3$, the diagonal matrix elements vary as $U_{mmmm}=3.84$, 3.39, 2.94, 3.39, and 3.48 eV for $m=xy$, yz, $3z^2-r^2$, zx, and x^2-y^2, respectively.

After the construction, the model (1) is solved in the HF approximation.[10]

TABLE I. Averaged values of the Coulomb interaction U, exchange interaction J, and nonsphericity B, obtained from the fitting of matrix elements $U_{mm'm''m'''}$. All parameters are measured in electron volts.

Compound	U	J	B
$PbVO_3$	1.57	0.84	0.08
$BiCoO_3$	2.38	0.90	0.09

III. RESULTS AND DISCUSSIONS

A. Qualitative analysis based on the spin model

The existence of the spin-spiral states in noncentrosymmetric perovskites can be understood in the framework of the spin model,[14]

$$\hat{\mathcal{H}}_S=-\sum_{\langle ij\rangle}J_{ij}\boldsymbol{S}_i\boldsymbol{S}_j+\sum_{\langle ij\rangle}\mathbf{d}_{ij}[\boldsymbol{S}_i\times\boldsymbol{S}_j]+\sum_i\boldsymbol{S}_i\hat{\tau}_{ii}\boldsymbol{S}_i \qquad (2)$$

(where J_{ij} is the isotropic exchange interaction, $\mathbf{d}_{ij}$ is the vector of antisymmetric Dzyaloshinskii-Moriya interactions, and $\hat{\tau}_{ii}$ is the single-ion anisotropy tensor), which can be obtained by mapping the electronic model (1) onto the spin one and integrating out all degrees of freedoms but spins. It can be done by different methods. One possibility is to consider the perturbation-theory expansion with respect to the infinitesimal spin rotations and SOI near the nonrelativistic ground state in the HF approximation.[15] In the following, the results of such a method are denoted by the symbols "inf." Moreover, for the d^1 configuration of $PbVO_3$, one can consider the theory of superexchange interactions in the second order with respect to the transfer integrals (in the following denoted by the symbol "set").[16]

Then, neglecting the single-ion anisotropy term for awhile, the energy of (classical) spin spiral in the zx plane,

$$\langle\boldsymbol{S}_i\rangle=S(\sin\mathbf{qR}_i,0,\cos\mathbf{qR}_i)$$

($\mathbf{R}_i$ being the radius vector of the site i), is given by

$$E(\mathbf{q})=-\sum_i\left(J_{0i}\cos\mathbf{qR}_i-d_{0i}^y\sin\mathbf{qR}_i\right),$$

and the spin-spiral vector $\mathbf{q}=(q_x,\pi/a,0)$ in the ground state should correspond to the minimum of $E(\mathbf{q})$.

TABLE II. Isotropic Heisenberg interactions (measured in meV) for $PbVO_3$ and $BiCoO_3$. Notations of the atomic sites are explained in Fig. 1. Results of the superexchange theory are denoted by the symbols set. Results for infinitesimal spin rotations near the nonrelativistic ground state are denoted by the symbols inf.

Bond	$PbVO_3$ (set)	$PbVO_3$ (inf)	$BiCoO_3$ (inf)
1-2	−49.86	−44.71	−9.65
1-3	−3.63	−0.64	−0.15
1-4	4.76	3.20	−0.91
1-5	3.94	1.25	−1.19
1-6	3.61	1.25	−0.07

TABLE III. Nonvanishing parameters of Dzyaloshinskii-Moriya interactions $\mathbf{d}_{ij} = (d^x_{ij}, d^y_{ij}, d^z_{ij})$ (measured in meV) for $PbVO_3$ and $BiCoO_3$. Notations of atomic sites and the coordinate frame are explained in Fig. 1. Other parameters are equal to zero. Results of the superexchange model are denoted by the symbols *set*. Results for infinitesimal spin rotations near the nonrelativistic ground state are denoted by the symbols *inf*. Note that Dzyaloshinskii-Moriya interactions vanish in bond 1-3 due to symmetry constraints.

Parameters	$PbVO_3$ (*set*)	$PbVO_3$ (*inf*)	$BiCoO_3$ (*inf*)
d^y_{12}	−0.98	−0.77	−0.13
$d^y_{14} = -d^x_{14}$	0.39	0.17	0
d^y_{15}	−0.11	−0.04	0
$d^y_{16} = -d^x_{16}$	−0.01	−0.03	0

Obviously, the isotropic exchange interactions (J_{0i}) will tend to establish a collinear spin structure with $\mathbf{qR}_i = 0$ or π, while Dzyaloshinskii-Moriya interactions (d^y_{0i}) will deform this structure and will make it incommensurate.[14] The Dzyaloshinskii-Moriya interactions are also responsible for the asymmetry between right-handed ($q_x > 0$) and left-handed ($q_x < 0$) spin-spiral states, which is manifested in the inequality $E(\mathbf{q}) \neq E(-\mathbf{q})$.

Parameters of isotropic exchange interactions (J_{ij}) are listed in Table II. We note that the schemes *set* and *inf*, in the case of $PbVO_3$, provide very similar results. This seems to be reasonable because, if the orbital configuration is quenched by the crystal field, the spin model (2) is well defined, and different computational schemes should yield similar model parameters (of course, provided that $|\hat{t}_{ij}/U| \ll 1$ and the scheme *set* makes sense). The magnetic transition temperature, evaluated in the RPA (see Ref. 16 for details) for the G- and C-type AFM states, is on the order of 200 and 600 K for $PbVO_3$ and $BiCoO_3$, respectively. The experimental Néel temperature for $BiCoO_3$ is 470 K.[3] The situation in $PbVO_3$ is rather controversial. On one hand, the results of the neutron powder-diffraction experiment are not conclusive because their interpretation strongly depends on the magnetic structure, which was *assumed* for the analysis of the experimental data.[4] On the other hand, the magnetic susceptibility of $PbVO_3$ does display a broad maximum at around 200 K, which could be regarded as the sign of an antiferromagnetism. Moreover, the G-type AFM order was proposed for the thin films of $PbVO_3$ below 130 K.[17]

Parameters of Dzyaloshinskii-Moriya interactions are shown in Table III. They are at least 1 order of magnitude smaller than J_{ij} for the same bonds.

Using these parameters, the spin-spiral vector q_x can be estimated as $q_x a = \pi - \Delta\phi$ (a being the lattice parameter in the xy plane), where $\Delta\phi = 6 \times 10^{-3}\pi$ and $4 \times 10^{-3}\pi$ for $PbVO_3$ and $BiCoO_3$, respectively. Thus, by considering only J_{ij} and $\mathbf{d}_{ij}$, both materials are expected to form spin-spiral structures, involving more than 100 unit cells. As we see below, this scenario indeed holds for $PbVO_3$ but not for $BiCoO_3$.

The main difference between $PbVO_3$ and $BiCoO_3$ is in the behavior of the single-ion anisotropy $\hat{\tau}_{ii}$. For the $S = 1/2$ compound $PbVO_3$, $\hat{\tau}_{ii}$ is expected to be zero as the consequence of fundamental Kramers degeneracy for the odd-electron systems. Particularly, the ground state of the self-interaction free ion V^{4+} is the Kramers doublet. Therefore, the rotation of spin corresponds to the unitary transformation of the wave function within this doublet without any energy cost. The situation is completely different for the $S = 2$ (or even-electron) compound $BiCoO_3$: The Kramers theorem is no longer applicable, which formally allows for the finite $\hat{\tau}_{ii}$. This statement can be verified by direct calculations of the anisotropy energies $\Delta E = E_{\parallel} - E_{\perp}$ (where the symbols "$\parallel$" and "$\perp$" correspond to the spin configurations, where $\langle \boldsymbol{S}_i \rangle$ is parallel and perpendicular to the tetragonal z axis). In the C-type AFM state, it yields $\Delta E = 0.02$ and -5.63 meV per formula unit for $PbVO_3$ and $BiCoO_3$, respectively. Moreover, the main contribution to ΔE indeed originates from the single-ion anisotropy. This can be seen by repeating the same calculations in the atomic limit (and enforcing $\hat{t}_{ij} = 0$ for all $i \neq j$), which yields $\Delta E = 0$ and -5.86 meV per formula unit for $PbVO_3$ and $BiCoO_3$, respectively. Small deviations from the atomic limit are due to intersite ($i \neq j$) anisotropic interactions $\hat{\tau}_{ij}$, which can be evaluated in the *set* model and are at least one order of magnitude smaller than $\mathbf{d}_{ij}$.[16] Using obtained values of ΔE and the symmetry considerations, nonvanishing parameters of the single-ion anisotropy tensor in $BiCoO_3$ can be estimated as $\tau^{xx}_{ii} = \tau^{yy}_{ii} = -\frac{1}{2}\tau^{zz}_{ii} = 0.49$ meV. Thus, we are dealing with the following hierarchy of magnetic interactions $|J_{ij}| \gg |\hat{\tau}_{ij}| \gg |\mathbf{d}_{ij}|$. It means that the formation of the spin-spiral state in $BiCoO_3$ is affected strongly by the single-ion anisotropy, which tends to restore the collinear spin structure by aligning the magnetic moments either parallel or antiparallel to the z axis. Of course, the final answer about the form of the magnetic ground state in $PbVO_3$ and $BiCoO_3$ can be obtained only on the basis of detailed calculations, which we discuss in the next section.

B. Solution of the electronic model

In this section, we present the results of extensive HF calculations for large supercells, which allow for the spin-spiral solutions with $q_x a = \pi(|L| - 1)/L$, where $|L|$ is the number of cells along the x axis: $L > 0$ and < 0 correspond

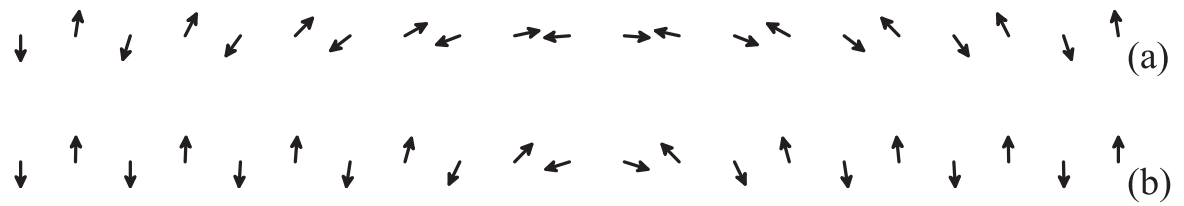

FIG. 3. Spin magnetic structure along the x directions in the case of (a) $PbVO_3$ and (b) $BiCoO_3$ as obtained in the HF calculations for $L = 21$. Here, x is the horizontal axis, and z is the vertical one.

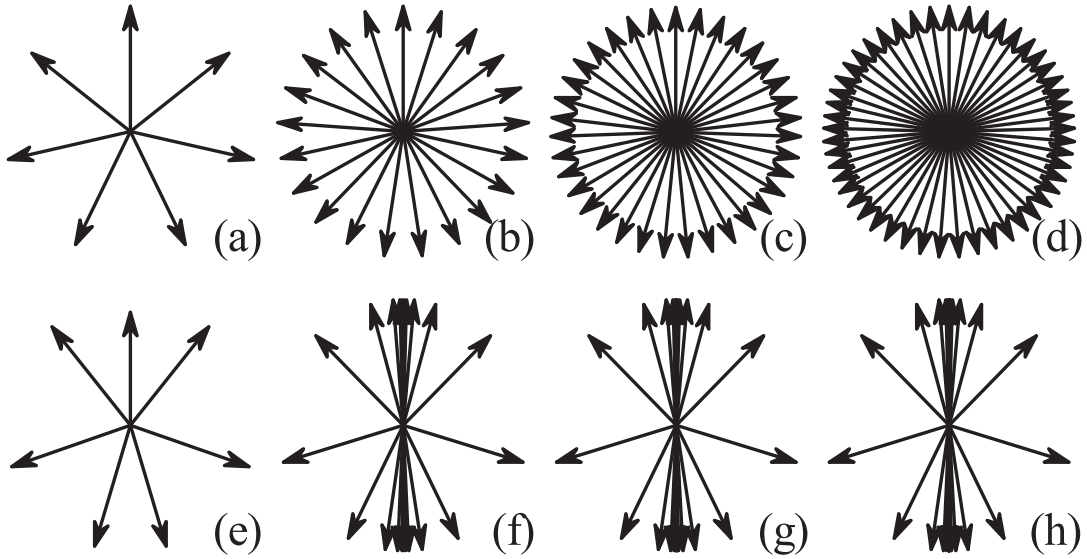

FIG. 4. Distribution of the spin magnetic moments (as if they were brought to the same origin) in the xz plane of $PbVO_3$ (top) and $BiCoO_3$ (bottom): results of HF calculations for $L = 7$ [(a) and (e)], $L = 21$ [(b) and (f)], $L = 35$ [(c) and (g)], and $L = 49$ [(d) and (h)]. Here, x is the horizontal axis, and z is the vertical one.

to the right- and left-handed alignment, respectively, and the collinear C-type AFM state is realized in the limit $|L| \to \infty$. The main results are summarized in Figs. 3 and 4. One clearly can see that there is a big difference between $PbVO_3$ and $BiCoO_3$. $PbVO_3$ tends to form a homogeneous spin-spiral state where the angle between neighboring magnetic moments along the x axis remains constant (small deviations are caused by weak intersite anisotropy effects). On the contrary, due to the large single-ion anisotropy, the spin-spiral configurations in $BiCoO_3$ strongly are deformed, and the moments are bunched around the z axis [Figs. 4(f)–4(h)]. The so-called bunching effect was well known for magnetic rare-earth metals and already was discussed more than 40 years ago.[18] Thus, within the considered geometry, $BiCoO_3$ tends to form an inhomogeneous magnetic state, which corresponds to the (nearly) collinear AFM alignment in the wide part of the supercell, except the small domain wall where the spins undergo the reorientation within the area of about ten unit cells. The latter solutions were obtained for odd numbers of cells L, which, in the AFM lattice, results in the formation of the domain-wall defect. For even L, the HF equations converge to the C-type AFM state. The spin pattern in the

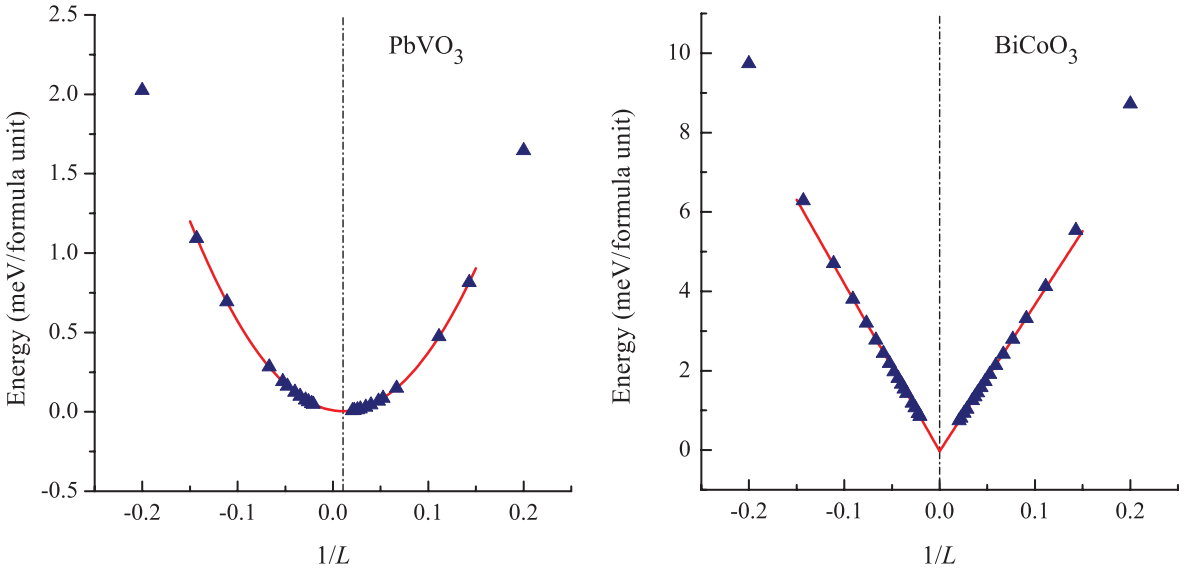

FIG. 5. (Color online) Total energies versus $1/L$ as obtained in the HF approximation for $PbVO_3$ (left) and $BiCoO_3$ (right). Calculated points are denoted by symbols. The solid line is the results of interpolation $E = A/L + B/L^2$ in the case of $PbVO_3$ (where $A = -0.99$ meV and $B = 46.36$ meV) and $E = A/L$ in the case of $BiCoO_3$ (where $A = -42.22$ meV for $L < 0$ and $A = 36.94$ meV for $L > 0$). The location of the total energy minimum is shown by the dot-dashed line.

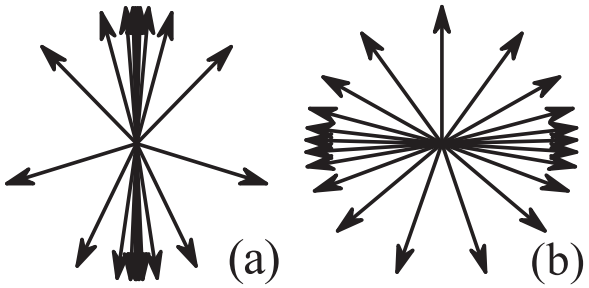

FIG. 6. Distribution of the spin magnetic moments (as if they were brought to the same origin), obtained in the HF calculations for $L = 21$. Left panel (a) shows results for the regular $BiCoO_3$, including all six valence electrons. Right panel (b) shows results for the hypothetical system, which has the same parameters of the electronic model but only one valence electron (and, therefore, no single-ion anisotropy term). Here, x is the horizontal axis, and z is the vertical one.

domain wall is well reproduced for $L = 21$ (Fig. 4). For larger cells, the additional spins participate in the formation of the AFM regions and are either parallel or antiparallel to the z axis, leading to tiny changes in Figs. 4(f)–4(h), which practically are not distinguishable to the eye.

Results of total energy calculations (Fig. 5) are well consistent with the above finding. As expected for the spin-spiral states, the dependence of the total energy on $1/L$ in the case of $PbVO_3$ is well described by the parabola. Due to the Dzyaloshinskii-Moriya interactions, there is a small asymmetry of the total energy with respect to the inversion $L \to -L$ of chirality of the spin spiral. Thus, the total energy minimum, obtained from the extrapolation, corresponds to the spin-spiral ground state with $L \approx 94$. On the contrary, the total energy of $BiCoO_3$ is a linear function of $1/L$. This is because of the localized character of the domain wall, for which the total energy (divided by the total number of cells) is expected to scale as $1/L$. Thus, the minimum corresponds to the collinear C-type AFM ground state ($|L| \to \infty$) in which the total energy exhibits the derivative discontinuity. Nevertheless, even in this case, the total energy has different slopes in the regions $L > 0$ and $L < 0$, again, due to the difference between right- and left-handed spin-spiral alignments in the domain wall.

The crucial role of the single-ion anisotropy in the formation of the easy-axis C-type AFM ground state can be illustrated by repeating supercell calculations for $BiCoO_3$ with the same parameters of the electronic model but with a different number of valence electrons: 1 instead of 6. Thus, according to the Kramers theorem, the single-ion anisotropy should vanish, similar to $PbVO_3$. The results for $L = 21$ are shown in Fig. 6, in comparison with regular $BiCoO_3$, including all six valence electrons. There are two types of effects. First, as already discussed in Sec. II, the effects of the SOI are larger in $BiCoO_3$ in comparison with $PbVO_3$. Therefore, intersite anisotropic interactions become stronger. In the hypothetical single-electron $BiCoO_3$, it is reflected in some bunching of magnetic moments around the horizontal x axis (similar bunching exists in $PbVO_3$—Fig. 4, but the effect is considerably weaker). Second, the easy-axis alignment in $BiCoO_3$ is related solely to the single-ion anisotropy term. As long as it is absent in the hypothetical single-electron $BiCoO_3$, the spin magnetic moments start to regroup around the x axis.

IV. CONCLUSIONS

Being based on the results of the low-energy electronic model, derived from the first-principles electronic structure calculations, we analyzed possible magnetic structures of two noncentrosymmetric perovskites $PbVO_3$ and $BiCoO_3$. We argued that, despite structural similarities, the magnetic behavior of these two materials is expected to be very different. $PbVO_3$, with spin $S = 1/2$, should form a long-periodic spin-spiral state, which results from the competition between isotropic exchange and Dzyaloshinskii-Moriya interactions in the noncentrosymmetric crystal structure. Due to the Kramers degeneracy, the single-ion anisotropy does not operate in $PbVO_3$. However, the latter is expected to play a major role in $BiCoO_3$ with spin $S = 2$. Particularly, the single-ion anisotropy suppresses the noncollinear spin-spiral alignment in $BiCoO_3$ and enforces the formation of the C-type AFM ground state in agreement with the experiment.[3] In this sense, this paper is an illustration of how fundamental properties of the matter (such as the Kramers theorem) can be used for the analysis of materials science properties.

We also believe that this funding has a direct implication on the properties of multiferroic manganites, which also have spin $S = 2$ and large single-ion anisotropy.[15] Therefore, the numerous claims about the spin-spiral ground state of these compounds, and related to its improper ferroelectric activity, should be taken cautiously. Again, due to the large single-ion anisotropy, the ground state of manganites is not necessarily the spin spiral, which prompts a search for an alternative mechanism of multiferroicity in these compounds.[12]

*SOLOVYEV.Igor@nims.go.jp

[1]D. Lebeugle, D. Colson, A. Forget, M. Viret, A. M. Bataille, and A. Gukasov, Phys. Rev. Lett. **100**, 227602 (2008).
[2]A. A. Belik, M. Azuma, T. Saito, Y. Shimakawa, and M. Takano, Chem. Mater. **17**, 269 (2005).
[3]A. A. Belik, S. Iikubo, K. Kodama, N. Igawa, S.-I. Shamoto, S. Niitaka, M. Azuma, Y. Shimakawa, M. Takano, F. Izumi, and E. Takayama-Muromachi, Chem. Mater. **18**, 798 (2006).
[4]R. V. Shpanchenko, V. V. Chernaya, A. A. Tsirlin, P. S. Chizhov, D. E. Sklovsky, E. V. Antipov, E. P. Khlybov, V. Pomjakushin, A. M. Balagurov, J. E. Medvedeva, E. E. Kaul, and C. Geibel, Chem. Mater. **16**, 3267 (2004).
[5]A. A. Tsirlin, A. A. Belik, R. V. Shpanchenko, E. V. Antipov, E. Takayama-Muromachi, and H. Rosner, Phys. Rev. B **77**, 092402 (2008).
[6]Y. Uratani, T. Shishidou, F. Ishii, and T. Oguchi, Jpn. J. Appl. Phys. **44**, 7130 (2005).
[7]D. J. Singh, Phys. Rev. B **73**, 094102 (2006).
[8]I. Dzyaloshinsky, J. Chem. Phys. Solids **4**, 241 (1958); T. Moriya, Phys. Rev. **120**, 91 (1960).

[9]H. Katsura, N. Nagaosa, and A. V. Balatsky, Phys. Rev. Lett. **95**, 057205 (2005); M. Mostovoy, *ibid.* **96**, 067601 (2006); I. A. Sergienko and E. Dagotto, Phys. Rev. B **73**, 094434 (2006).

[10]I. V. Solovyev, J. Phys.: Condens. Matter **20**, 293201 (2008).

[11]I. V. Solovyev and Z. V. Pchelkina, Phys. Rev. B **82**, 094425 (2010).

[12]I. V. Solovyev, Phys. Rev. B **83**, 054404 (2011).

[13]See Supplemental Material at http://link.aps.org/supplemental/10.1103/PhysRevB.85.054420 for parameters of the crystal field, transfer integrals, and matrices of Coulomb interactions.

[14]I. Sosnowska and A. K. Zvezdin, J. Magn. Magn. Mater. **140–144**, 167 (1995).

[15]I. Solovyev, N. Hamada, and K. Terakura, Phys. Rev. Lett. **76**, 4825 (1996).

[16]I. V. Solovyev, New J. Phys. **11**, 093003 (2009).

[17]A. Kumar, L. W. Martin, S. Denev, J. B. Kortright, Y. Suzuki, R. Ramesh, and V. Gopalan, Phys. Rev. B **75**, 060101(R) (2007).

[18]W. C. Koehler, J. W. Cable, M. K. Wilkinson, and E. O. Wollan, Phys. Rev. **151**, 414 (1966); G. P. Felcher, G. H. Lander, T. Arai, S. K. Sinha, and F. H. Spedding, Phys. Rev. B **13**, 3034 (1976).